Steps on subliming Si(111) surfaces

Steps on subliming Si(111) surfaces

Yoshikazu Homma and Paul Finnie

NTT Basic Research Laboratories, Atsugi, Kanagawa 243-0198, Japan

Abstract. We investigated sublimation-related phenomena and dynamics of atomic steps on Si(111) surfaces that were atomically flat on a large scale ($\sim$100 $\times$ 50 μm) by ultrahigh-vacuum scanning electron microscopy. Step spacing during step-flow sublimation was analysed as a measure of the adatom diffusion length, and compared between a normal Si(111) and a heavily boron-doped Si(111). The spacing showed a transition-like increase, which is related to incomplete surface melting. The step-flow velocity was obtained for the ultralarge terraces. The step–step interactions were directly examined by making two steps collide.

1. Introduction

Atomic steps on a growing surface are well described by the classical model of epitaxial growth by Burton, Cabrera and Frank (BCF) [1]. This model basically can be extended to steps on subliming surfaces. However, there are complications on a subliming surface due to the presence of both adatoms and advacancies [2]. Experimentally, the available methods for *in situ* characterizations are limited, because sublimation occurs at high temperatures for metals and semiconductors. So far, reflection electron microscopy has been successfully applied to observe the steps on subliming surfaces in real time [3–5]. Alternatively, sublimation-related phenomena can be observed by quenching the surface from a high temperature. An ultralarge terrace created on the Si(111) surface [6] is especially useful for observing such phenomena: it enables the analysis of atomic step motion even after quenching, because the terrace size and step spacing are far beyond the step displacement during quenching. The ultralarge terrace provides a very good platform for testing theories.

In this paper, we describe the behaviour of atomic steps on subliming Si(111) surfaces based on the observation of ultralarge terraces by ultrahigh-vacuum scanning electron microscopy. We compare the atomic step distributions and sublimation modes between normal Si(111) and heavily boron-doped Si(111) surfaces. The heavily doped surface retains a $\sqrt{3} \times \sqrt{3}$ structure up to 1100 °C, while the normal Si(111) surface exhibits '1 $\times$ 1' in the entire sublimation regime. We measure step velocities and compare them to the theory. By making steps collide, we directly probe the length scale and strength of step–step interactions.

2. Ultralarge terrace formation and step observation

At high temperatures, the Si(111) surface is covered with adatoms released from steps. New adatoms are continuously released from the steps to compensate for the decrease in the adatom
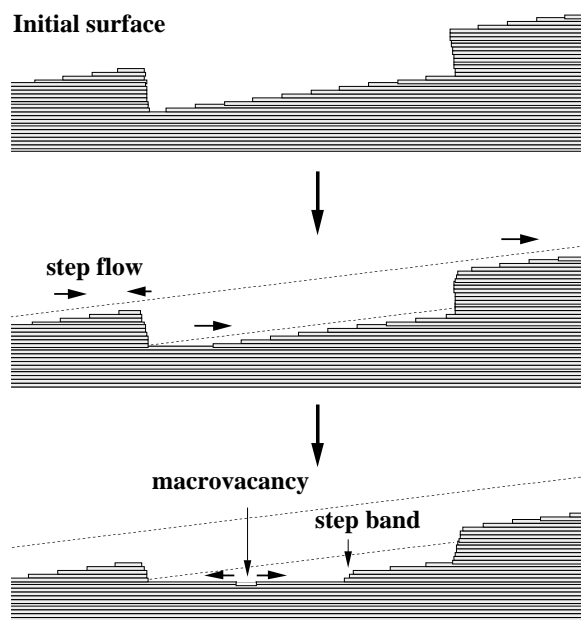
Initial surface

Figure 1. Schematic illustration of expansion of the bottom terrace in a crater by step-flow sublimation.

concentration due to desorption, causing step retraction. On a vicinal surface, steps move in the same direction, which maintains the initial vicinality. On the other hand, at the bottom of a crater, as schematically shown in figure 1, the steps surrounding the lowest terrace of the crater move so as to expand the terrace area by step-flow sublimation. (Actually, when the bottom terrace is much smaller than the adatom diffusion length, the filling in of the bottom terrace dominates, not step retraction. In the present case, filling in occurs only in the initial stage. Details will be reported elsewhere.) When the terrace width becomes large enough, steps are newly created at the centre of the widest part of the (111) plane due to precipitation of vacancies (macrovacancy formation) [7]. The plane expands until one of the top edges of the crater (the left edge in figure 1) disappears by sublimation, and can reach to a width of more than 50 μm.

Step behaviour was investigated using such ultralarge (111) terraces. We used a lightly boron-doped Si(111) wafer ($\sim$5 Ω cm, 0.15° miscut) as a normal Si(111) substrate, and a heavily boron-doped Si(111) wafer ($\sim$0.001 Ω cm, 0.3° miscut). A square crater with sides of 150 μm $\times$ 150 μm and a depth of about 1 μm was formed on the surfaces by O_2^+ beam raster-scanning with a secondary ion mass spectrometry (SIMS) instrument. Samples with craters were introduced into an ultrahigh-vacuum electron microscope (UHV-SEM) and resistively heated in the UHV-SEM chamber. To image steps on a wide plane, we decorated the atomic steps with 7 $\times$ 7 reconstruction domains by radiation quenching the surface. On the quenched surface, continuous 7 $\times$ 7 regions nucleated only at steps, thus the steps appeared as brighter lines in SEM images [7]. The heavily boron-doped Si(111) exhibited the $\sqrt{3} \times \sqrt{3}$ reconstruction up to 1100 °C. The 7 $\times$ 7 reconstruction never appeared on this surface, but atomic steps on an ultralarge terrace could be imaged by quenching the sample from a higher temperature. The $\sqrt{3} \times \sqrt{3}$ structure also nucleated from steps and could not expand to cover the whole surface during rapid quenching. Therefore, the steps on the heavily boron-doped
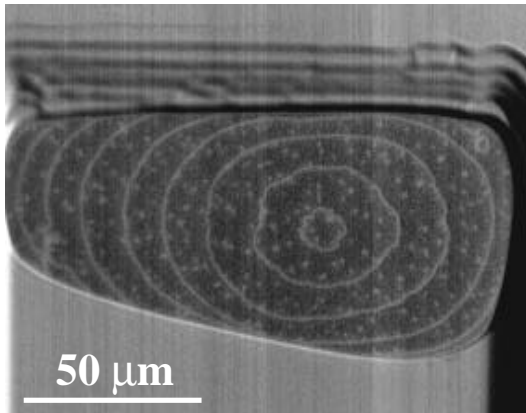
Figure 2. SEM image of the step distribution on a wide (111) plane quenched from 1180 °C. Brighter regions are 7 × 7 domains nucleated at steps during quenching.

(111) surface could be visualized by SEM in just the same way as the 7 × 7 decoration. These reconstruction domains were identified using reflection high-energy electron diffraction in the UHV-SEM.

3. Step distribution on subliming terrace

Figure 2 shows an SEM image of the normal Si(111) surface quenched from 1180 °C. Concentric steps are seen. The steps have about a 10 μm spacing and descend toward the centre. This concentric shape is formed because new steps are created at the centre of the (111) plane and steps expand due to sublimation in a step-flow manner. The step–step spacing is determined by the adatom diffusion length. According to the analysis of subliming Si surfaces by Pimpinelli and Villain [2], macrovacancies nucleate on a vicinal surface when the step–step spacing l roughly satisfies

$$l > \lambda_s \gamma / kT \tag{1}$$

where λ_s is the adatom diffusion length before desorption, γ is the step stiffness, k is the Boltzmann constant and T is the absolute temperature. On the (111) surface, γ is of the order of kT. Thus, inequality (1) implies macrovacancies nucleate when the terrace size is of the order of the adatom diffusion length. The model of Pimpinelli and Villain is for a terrace between two parallel steps, while in the present case the bottom terrace is circular. In spite of this difference, the criterion for macrovacancy nucleation expressed by inequality (1) can be used as a rough estimation, i.e. macrovacancies nucleate when the radius of the terrace becomes larger than the order of the adatom diffusion length. Thus, the step spacing in figure 2 can be regarded as roughly the adatom diffusion length.

The step spacing depends on temperature. Figure 3 shows that, below 1200 °C, the step spacing decreases from ∼50 to ∼10 μm with increasing temperature. This decrease is attributed to the decrease in the adatom diffusion length due to the increase in the desorption probability [7]. The spacing, however, shows a transition-like increase around 1200 °C, then, above 1240 °C, decreases again. The transition-like increase in the step spacing suggests surface structure changes in some way. One likely change at such a high temperature is 'incomplete surface melting', which is a disordering of the first monolayer and has actually been observed on Ge(111) near the melting point [8, 9]. Recently, Hibino *et al* confirmed incomplete melting on Si(111) using reflection high-energy electron diffraction and medium-energy ion scattering spectroscopy [10].
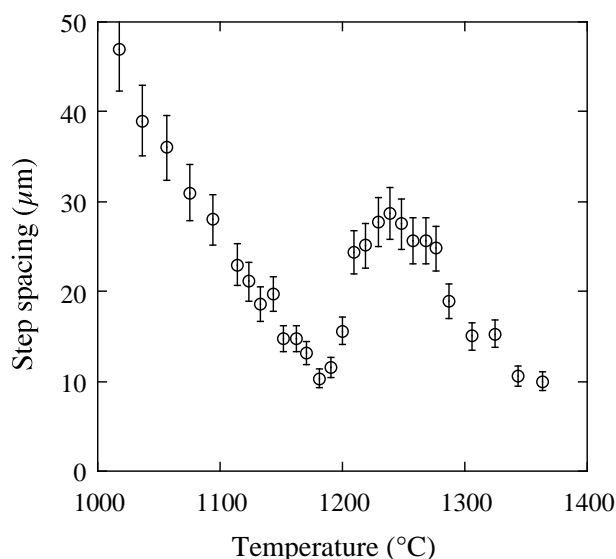
Figure 3. Temperature dependence of step spacing on the normal Si(111).

4. Sublimation of heavily boron-doped Si(111) surface

4.1. Step spacing on an ultralarge (111) terrace

Similar sublimation phenomena were observed on a heavily boron-doped Si(111) surface, but the transition temperature and the behaviour at lower temperatures were different from those for the normal Si(111) surface.

The surface images of the heavily boron-doped Si(111) exhibited three different features, depending on the temperature from which the sample was quenched. Figure 4 shows typical images for each temperature region, and the temperature dependence of the characteristic length, such as step spacing or 'denuded zone width' (see 4.2). Images (b) and (c) are basically similar to those of the normal Si(111) surface. Image (b) shows a step distribution in a concentric shape, similar to that in figure 2. This distribution appeared between 1100 and 1260 °C. However, the step spacing is small and the temperature dependence is not so steep compared to those on the normal Si(111) surface shown in figure 3. The step distribution in image (c) corresponds to that of an incompletely melted surface. The transition occurred at 1260 °C, 60 degrees higher than for the normal Si(111). The step spacing is tripled compared to image (b), and small circular steps can be seen. These small circular steps are formed between concentric steps during the quenching process [7]. Above the transition temperature, the step spacing is almost the same for both the heavily-doped and normal samples [11].

The changes observed on the heavily boron-doped surface were attributed to the higher diffusion barrier caused by boron at subsurface sites [11]. Boron atoms are located at substitutional S_5 sites in the second layer and stabilize T_4-site adatoms on a $\sqrt{3} \times \sqrt{3}$ B surface [12]. Above 1100 °C, the surface no longer retains the $\sqrt{3} \times \sqrt{3}$ reconstruction. However, it is speculated that some boron atoms still remain at S_5 sites at temperatures between 1100 and 1260 °C. It follows then that the lifetime of adatoms at T_4 sites may be longer, although adatoms do not stay still at T_4 sites. The longer lifetime would make the adatom diffusion barrier higher. In addition, it could contribute to step stiffness and make the incomplete melting transition temperature higher. Since the incomplete melting transition is the disordering of
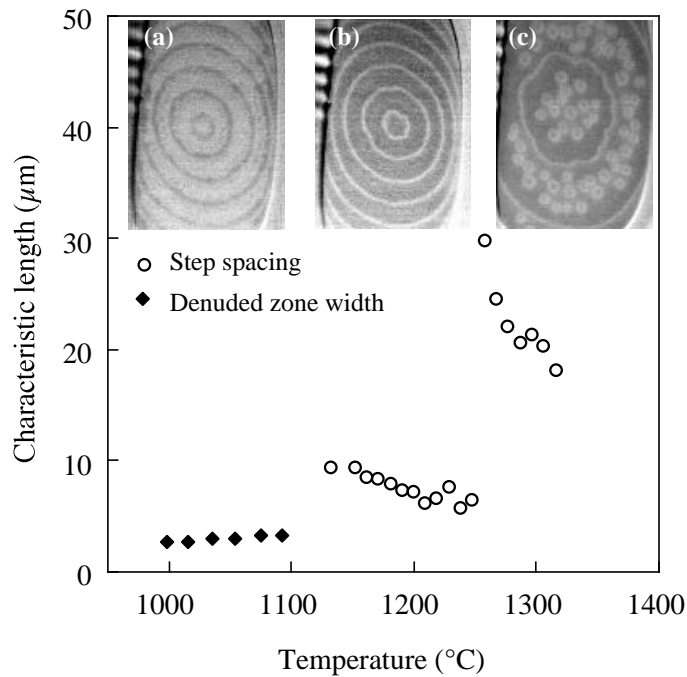
Figure 4. Temperature dependence of characteristic length on the heavily boron-doped Si(111) surface. Insets: typical SEM images of a wide (111) plane in each temperature range. Images were taken after quenching from (a) 1040, (b) 1230 and (c) 1270 °C. Brighter regions are $\sqrt{3} \times \sqrt{3}$ domains nucleated at steps during quenching.
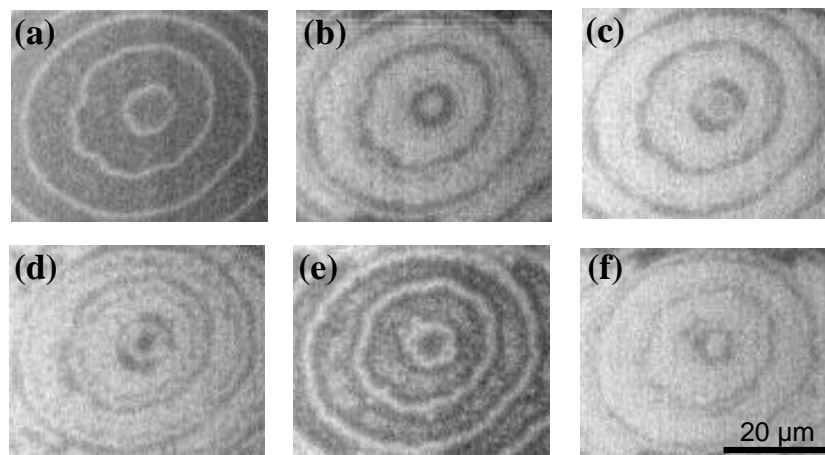

Figure 5. SEM contrast change during sublimation of a wide (111) plane on the heavily boron-doped Si(111) at 1056 °C. The initial surface (a) was prepared by quenching from 1220 °C. Images were then taken by repeatedly heating and quenching. The cumulative heating times were: (b) 20, (c) 50, (d) 65, (e) 80 and (f) 95 s. Images from (a) to (e) correspond to one period.

the first monolayer, boron atoms do not locate at the subsurface sites after the transition. Consequently, the surface property should be the same as that of the normal surface. This explains the same step spacing for both samples after the incomplete melting transition.

4.2. Sublimation mode change

The surface shown in image (a) of figure 4 appeared between 1000 and 1100 °C (the '1 × 1'– $\sqrt{3} \times \sqrt{3}$ transition temperature). The contrast in image (a) is reversed with respect to image (b). This contrast inversion is due to vacancy island formation on the terraces. Successive images taken during heating clarify the phenomenon occurring. The images in figure 5 were obtained after repeated heating and quenching. The initial surface (a) was prepared by quenching from 1220 °C, then the sample was heated to 1056 °C. The contrast inverts in the early stage and stays inverted up until 70 s of heating (b)–(d). Then, it returns to one similar to the initial one (e). This contrast change is repeated upon further heating. The step shapes remain almost the same throughout this cycle.

This phenomenon is interpreted as layer-by-layer sublimation with monolayer vacancy-island formation. The SEM image remained almost the same even when the area of vacancy islands increased during sublimation, because the $\sqrt{3} \times \sqrt{3}$ area nucleated during quenching is larger than the vacancy islands. However, upon monolayer sublimation, the surface smoothed again, resulting in contrast recovery. During the contrast inversion period, darker zones were seen near the steps. These are denuded zones where no vacancy island exists because the steps act as sinks for vacancies. The zone width is plotted in figure 4. Though the width of a denuded zone is larger for a lower terrace than for an upper one, it is of the order of several micrometres and much smaller than the terrace size. This indicates that the vacancy (or adatom) diffusion length on the $\sqrt{3} \times \sqrt{3}$ surface becomes smaller than that on the '1 × 1' surface, resulting in a sublimation-mode change from step flow to 2D-island formation in a wide terrace. The width of the denuded zone has very little temperature dependence at 1000–1100 °C as shown in figure 4. The reason the $\sqrt{3} \times \sqrt{3}$ structure appeared only near steps even below the $\sqrt{3} \times \sqrt{3}$ transition temperature, 1100 °C, may be that the $\sqrt{3} \times \sqrt{3}$ structure is imperfect on a terrace wider than the diffusion length of a vacancy (or adatom) in the temperature range of 1000–1100 °C. Below 1000 °C, the whole surface turned to a well ordered $\sqrt{3} \times \sqrt{3}$.

The occurrence of vacancy-island-nucleation-mode sublimation below 1100 °C means a decrease of adatom diffusion length to several micrometres [11]. An explanation for this is that the density of non-T_4 adatoms is so small on the $\sqrt{3} \times \sqrt{3}$ surface that T_4 adatoms play the major role in the adatom diffusion and advacancy creation in inequality (1). In this situation, the diffusion barrier of a T_4 adatom and, in turn, that of an advacancy, is high because of the closely packed T_4 adatom configuration. In contrast, a non-T_4 adatom can diffuse to a step or evaporate easily. Hence, the density of advacancies exceeds that of non-T_4 adatoms, which causes a high macrovacancy density on a wide terrace.

5. Sublimation rate

The sublimation rate of the heavily boron-doped sample can be precisely determined from the period of contrast change, such as shown in figure 5, in the temperature range from 1000 to 1100 °C. The period corresponds exactly to the sublimation of 1 bilayer (1.6×10^{15} atoms cm^{-2}). For the normal Si(111) sample, the sublimation rate was derived from step retraction velocity on a wide terrace at various temperatures. The results are shown in figure 6, which also plots previously reported values [5, 13, 14]. The sublimation rates for both samples agree within the experimental error and are consistent with the values measured at higher temperatures in the literature. Note that the sublimation rate shows no anomaly at the step-spacing transition temperature.
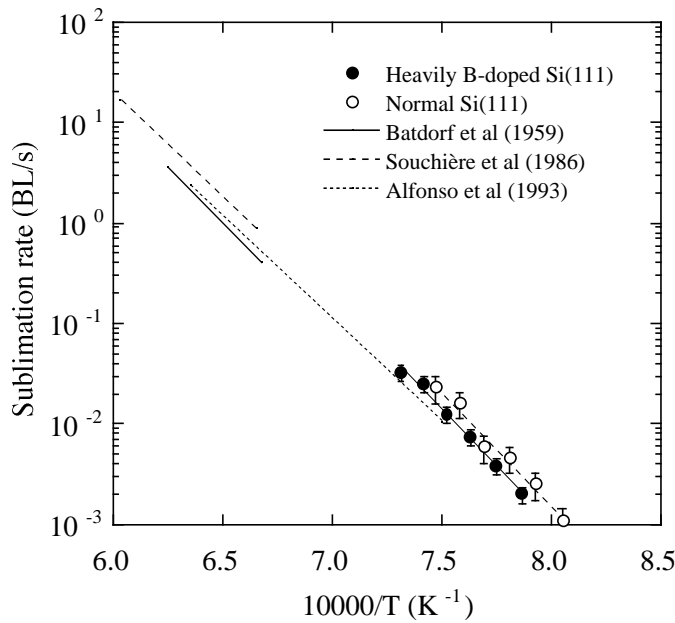
Figure 6. Arrhenius plot of sublimation rate (bilayers s^{-1}) for the heavily boron-doped Si(111) surface and normal Si(111) surface [11]. The heavily-doped data were derived from the period of SEM contrast change, such as shown in figure 5, while the normal surface data were obtained from the step retraction rate. Curves from [5], [13] and [14] are also shown.

It can be assumed that the sublimation rate depends very little on the boron concentration above 1100 °C, because even the sublimation rate of the $\sqrt{3} \times \sqrt{3}$ surface is almost the same as a normal '1 × 1' surface. The sublimation rate is expressed by

$$\nu = \nu_0 \exp[-(W_\nu + W_a)/kT] \tag{2}$$

where ν_0 is the atomic frequency, W_ν is the desorption barrier for adatoms and W_a is the adatom formation energy. The results in figure 6 indicate that $W_\nu + W_a (\sim 4.3 \text{ eV})$ barely changes for the heavily doped and normal Si(111) samples. Since W_a on the '1 × 1' surface is about 0.2 eV [2], $W_\nu \gg W_a$. It is also expected for the $\sqrt{3} \times \sqrt{3}$ surface that $W_\nu \gg W_a$. Hence, the results in figure 5 mean W_ν is almost the same for the heavily doped and normal Si(111) samples.

6. Step dynamics observed on a wide terrace

6.1. Step velocity

The ultraflat (111) terrace was utilized to investigate the dynamic processes of steps [15]. Step-flow motion during sublimation was analysed by annealing and quenching the surface successively. From images of concentric circular steps, each step edge position was traced and measured as a function of annealing time. The position of each successive crater edge was measured along a line from the edge of the ultraflat terrace to the original nucleation centre.

Nucleation of successive craters was completely regular. As the innermost crater reached the critical diameter—i.e. the step spacing described in equation (1)—a new crater was nucleated. The newly nucleated crater would expand, and the process would repeat after a fixed time interval.
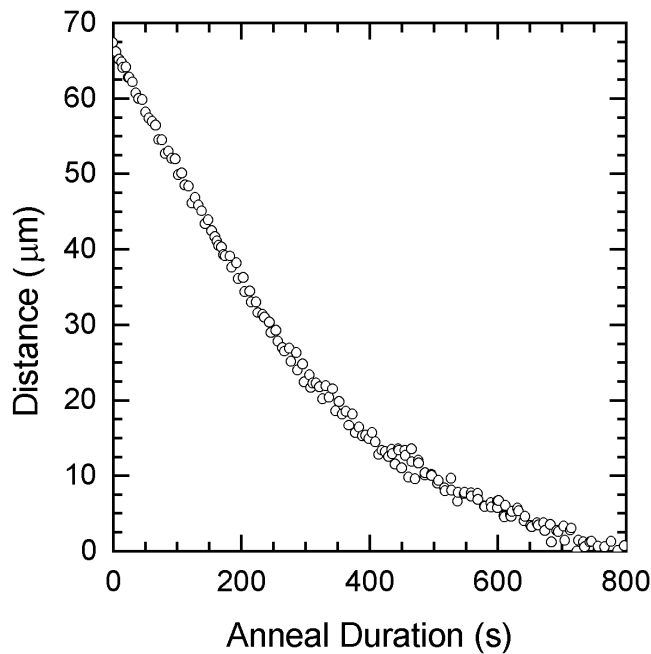
Figure 7. Evolution of circular steps during 1037 °C annealing on a wide (111) plane. The data from six successive concentric steps are combined into a single curve. The centre of the crater was located at 67.5 μm and the crater edge was at 0 μm.

A unique evolution curve was obtained by overlaying all the individual crater evolution curves [15]. This is done simply by time shifting each one by a multiple of the fixed time interval. Figure 7 shows an evolution curve obtained at 1037 °C annealing, with a nucleation time interval of about 145 s. When the step was newly nucleated it moved outward at a roughly constant rate. In contrast, as the step approached the outer edge of the ultraflat crater (located at the distance of 0 μm) it decelerated. Near this outer edge, steps bunched up as they decelerated.

Although the step spacing changes initially, the retraction velocity changes very little from its initial velocity of 170 ± 10 nm s^{-1}. In contrast, previous observations showed the velocity was proportional to the step spacing [3, 5]. However, those data were obtained at much smaller step spacings. This may be the first time a spacing-independent step velocity has been obtained, but, as described below, this constant velocity differs from the theoretically predicted saturation velocity.

In BCF theory, adatom coverage satisfies a diffusion equation and step velocities are determined by the net adatom flux at the step edge. In the original BCF formulation, there is a constant effective adatom coverage, θ_0, at the step edge. The resulting step velocity is

$$v = \lambda \frac{\theta_0}{\tau} \left[\tanh(w_L/2\lambda) + \tanh(w_U/2\lambda) \right] \tag{3}$$

where λ is the diffusion length, τ is the desorption time, w_L is the terrace width on the lower side of the step and w_U is the terrace width on the upper side of the step. Fitting this relation to the evolution curve results in $\tau/\theta_0 = 147 \pm 3$ s for $\lambda = 26$ μm [15].

From equation (3) it is seen that the velocity of an isolated step saturates. That is for $w_L, w_U \gg \lambda$ the hyperbolic tangents in (3) saturate to unity. The saturation velocity obtained using the fitting parameters is ∼340 nm s^{-1}, or about twice the nearly constant initial velocity

[15]. This is understandable since at early times the inner crater is very small, meaning its contribution to the velocity is also small, while the upper terrace is large, and so its contribution nearly saturates. It is difficult to observe a higher velocity, except transiently, because when the step spacing becomes larger than the diffusion length, new steps nucleate spontaneously [7].

6.2. Step collision

On the ultraflat terrace, the motion of individual steps can be observed, and so can the collision of two or more steps [15]. In collisions the interaction between steps can be probed directly. Several kinds of collision are possible by changing annealing conditions. When two opposing steps meet by retreating into each other, the collision is destructive, since the two steps annihilate one another, and a flat terrace remains. When two steps retreating in the same direction meet with one overtaking the other, the collision is constructive, resulting in a double atomic step. Here, only the results of a destructive collision will be described.

With the creation of multiple nucleation sites, it is possible to cause destructive step collisions. Two or more nucleation sites can be created intentionally by annealing at a high temperature such that the diffusion length becomes very short. Alternatively, they can be created by chance at lower temperatures, since occasionally an additional nucleation site may form.
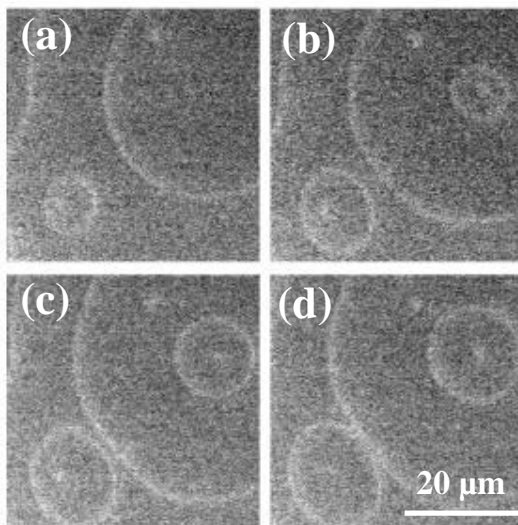

Figure 8. Destructive collision after various annealing durations: (a) 0 s, (b) 100 s, (c) 160 s and (d) 200 s total annealing at 998 °C.

Figure 8 is a time ordered sequence of frames showing the dynamics of a destructive collision. The circular craters are in the process of expanding. The largest crater is colliding with a smaller one originating from a separate nucleation site. As they approach one another the craters flatten, particularly in the case of the large one. Therefore, the interaction is repulsive. Step velocities at 1037 °C fell substantially when the spacing between colliding steps fell to ~4 μm.

In general terms, the flattening and deceleration can be understood with reference to equation (3). The velocity is an increasing function of terrace size on either side of the step. Thus step velocity is reduced on both sides of the terrace as the step edges approach one another and the terrace width falls below the diffusion length. The point of closest approach is slowed the most, so that the rest of the step catches up, leading to the flattening effect.

Recently, more general theories have included transparency of steps [16]. Steps are said to be transparent if they do not significantly modify the neighbouring adatom coverage. However, the relatively long-range interaction seen here is almost certainly diffusion mediated. That is, steps are modifying the local adatom coverage enough to influence the nearest step. Destructive collision experiments from 1000 to 1100 °C show the same flattening and so suggest that steps are not transparent [15].

Interestingly, the range, though long, is less than the measured diffusion length. This discrepancy is difficult to explain without a departure from the original BCF theory. Steps with some degree of transparency would be one plausible explanation. Future collision experiments should be able to quantify the transparency.

7. Summary

Atomic steps during sublimation have been analysed using *in situ* SEM observations of wide Si(111) planes created at the bottom of craters.

The step spacing on the plane depended on the heating temperature and reflects the adatom diffusion length. The step spacing transition occurred at 1200 °C on a normal Si(111) surface, which is considered to be evidence of incomplete surface melting. The step spacing on the heavily doped '1 × 1' surface was smaller than that on the normal '1 × 1' surface. In addition, the incomplete surface-melting transition of the heavily doped surface was 60 °C higher than that of the normal '1 × 1' surface. These findings were attributed to the segregation of boron, some of which might stay at S_5 sites even in the '1 × 1' phase above 1100 °C and reduce the adatom diffusion length. We also found that, below 1100 °C, the sublimation mode changed from step-flow to 2D vacancy-island nucleation on the wide terrace of the heavily doped surface. This might be due to a low mobility of T_4 adatoms on the $\sqrt{3} \times \sqrt{3}$ B surface.

The detailed motion of steps was studied on an ultralarge (111) terrace, allowing the measurement of fundamental parameters in BCF theory. A constant velocity was observed for widely spaced steps. Steps were made to undergo destructive collisions, which demonstrated that they interact repulsively and gave the range of interaction. This suggested that steps are not 'transparent'.

References

[1]   Burton W K, Cabrera N and Frank F C 1951 *Phil. Trans. R. Soc.* **243** 299
[2]   Pimpinelli A and Villain J 1994 *Physica* A **204** 521
[3]   Latyshev A V, Aseev A L, Krasilnikov A B and Stenin S I 1989 *Surf. Sci.* **213** 157
[4]   Latyshev A V, Aseev A L, Krasilnikov A B and Stenin 1990 *Surf. Sci.* **227** 24
[5]   Alfonso C, Heyraud J C and Métois J J 1993 *Surf. Sci. Lett.* **291** L745
[6]   Homma Y, Ogino T and Aizawa N 1996 *Japan. J. Appl. Phys.* **35** L241
[7]   Homma Y, Hibino H, Ogino T and Aizawa N 1997 *Phys. Rev.* B **55** R10 237
[8]   McRae E G and Malic R A 1987 *Phys. Rev. Lett.* **58** 1437
[9]   Denier van der Gon A W, Gay J M, Frenken J W M and van der Veen J F 1991 *Surf. Sci.* **241** 335
[10] Hibino H, Sumitomo K, Fukuda T, Homma Y and Ogino T 1998 *Phys. Rev.* B **58** 12 587
[11] Homma Y, Hibino H, Ogino T and Aizawa N 1998 *Phys. Rev.* B **58** 13 146
[12] Headrick R L, Robinson I K, Vlieg E and Feldman L C 1989 *Phys. Rev. Lett.* **63** 1253
      Bedrossian P, Meade R D, Mortensen K, Chen D M, Golovchenko J A and Vanderbilt D 1989 *Phys. Rev. Lett.* **63** 1257
      Lyo I-W, Kaxiras E and Avouris Ph 1989 *Phys. Rev. Lett.* **63** 1261
[13] Batdorf R L and Smits F M 1959 *J. Appl. Phys.* **30** 259
[14] Souchière J L and Thien Binh Vu 1986 *Surf. Sci.* **168** 52
[15] Finnie P and Homma Y 1999 *Phys. Rev. Lett.* **82** 2737
[16] Stoyanov S 1997 *Surf. Sci.* **370** 345